Eur Biophys J (1991) 19:109–118

European Biophysics Journal

Competitive blockage of the sodium channel by intracellular magnesium ions in central mammalian neurones

F. Lin [1], F. Conti [2], and O. Moran [1]

[1] Settore di Biofisica, Scuola Internazionale Superiore di Studi Avanzati (SISSA), Via Beirut 2–4, I-34014 Trieste, Italy
[2] Instituto di Cibernetica e Biofisica, C.N.R., Via Dodecaneso 33, I-16146 Genova, Italy

Received July 9, 1990/Accepted in revised form October 8, 1990

Abstract. The aim of this study was to determine from macroscopic current analysis how intracellular magnesium ions, Mg_i^{2+}, interfere with sodium channels of mammalian neurones. It is reported here that permeation across the sodium channel is voltage- and concentration-dependently reduced by Mg_i^{2+}. This results in a general reduction of sodium membrane conductance and an outward sodium peak current at large positive potentials. 30 m*M* Mg_i^{2+} leads to a negative shift of voltage dependence of sodium channel gating parameters, probably due to the surface potential change of the membrane. This shift alone is, however, insufficient to explain the reduction of outward sodium currents. The blockage by Mg_i^{2+} is decreased upon increasing intracellular or extracellular Na^+ concentration, which suggests that Mg_i^{2+} interferes with sodium permeation by competitively occupying sodium channels. Using a kinetic model to describe the sodium permeation, the dissociation constant (at zero membrane potential) of Mg_i^{2+} for the sodium channel has been calculated to be 8.65 ± 1.51 m*M*, with its binding site located at 0.26 ± 0.05 electrical distance from the inner membrane. This dissociation constant is smaller than that of Na_i^+, which is 83.76 ± 7.60 m*M* with its binding site located at 0.75 ± 0.23. The low dissociation constant of Mg_i^{2+} reflects its high affinity for the sodium channel.

Key words: Sodium channel – Patch clamp – Cerebellar granule cells – Intracellular magnesium

Introduction

Intracellular Mg^{2+} is involved in several cellular functions, by regulating various biochemical reactions (Strata and Benedetti 1988). The regulation of Mg_i^{2+} has been studied in different preparations (e.g. Altura and Altura 1985; Baker and Dipolo 1984). Intracellular Mg^{2+} is also known to interact with several ionic channels, such as the *N*-methyl-D-aspartate-activated channel (Johnson and Ascher 1990), the ATP sensitive potassium channel (Horie et al. 1987), the muscarinic potassium channel (Horie and Irisawa 1987), the inward rectifier potassium channel (Matsuda 1988), and calcium channels (White and Hartzell 1988).

The reduction of outward currents through the sodium channel, expressed in *Xenopus* oocytes from rat brain cDNA, has also been described (Pusch et al. 1989; Pusch 1990). The cerebellar granule cell in culture has been recognized as an excellent model for studying electrophysiological (e.g. Hockberger et al. 1987; Cull-Candy et al. 1989; Sciancalepore et al. 1989; Lin and Moran 1990) and biochemical (e.g. Levi et al. 1984; Nicoletti et al. 1987) properties of neurones, owing to the fact that it maintains the morphological and functional properties of native neurones (Levi et al. 1984). We have, therefore, investigated in detail the effect of Mg_i^{2+} on macroscopic Na^+ currents in cerebellar granule cells in order to study the possible kinetic mechanism of the Mg^{2+} blockage. From our results, we propose that Mg_i^{2+} blocks sodium channels by entering the sodium channel and binding to a site inside the pore with high affinity.

Methods

Cell preparation

Experiments were performed on cerebellar granule cells dissociated from eight days old Wistar rats, and prepared according to Levi and co-workers (1984). In order to diminish the problems of space-clamp produced by the neuritic processes growing, and of differences in the sodium channel expression during differentiation in vitro, cells were used only between 3 and 5 days in culture (DIC).

Bath solutions were (in millimolar): $CaCl_2$ 2, $CoCl_2$ 5, HEPES-NaOH (*N*-2-hydroxyethylpiperazine) 10 and NaCl 40, 60 and 100 respectively. Pipette solutions, dialyzing the intracellular compartment, had different Na^+ and Mg^{2+} concentration ($[Na^+]_i$, $[Mg^{2+}]_i$), as described

Offprint requests to: O. Moran

Table 1. Intracellular (pipette) solutions. Osmolarities of solutions were adjusted with *d*-glucose (see text)

Composition	15 Na^+ [m*M*]	20 Na^+ [m*M*]	30 Na^+ [m*M*]	30 Na^+ [m*M*]
NaCl	5	10	20	20
$MgCl_2$	0, 0.5, 1, 3, 7	0, 0.5, 1, 2, 3, 5, 7	0, 0.5, 1, 3, 7	30
CsF	110	105	95	70
EGTA[a]	11	11	11	11
HEPES-NaOH	10	10	10	10

[a] EGTA: Ethylenglycol-*bis*-β-amino-ethylether

in Table 1. Osmolarities of intracellular solutions were corrected to 295 mOsm and those of external solutions to 310 mOsm with *d*-glucose. In all solutions, pH was adjusted to 7.35. All experiments were performed at room temperature (17 to 21 °C).

Voltage clamp experiments

Ionic currents were measured in the whole-cell configuration of the patch-clamp technique (Hamill et al. 1981), using a standard patch-clamp amplifier (EPC-7, List Medical Electronics). Patch pipettes were pulled from borosilicate glass pipettes (Hilgenberg) and had resistances in the range of 2.5 to 4 *M*Ω after fire polishing, and determined with our intracellular/extracellular working solutions. In all experiments, potassium currents were negligible because of intracellular substitution of K^+ with Cs^+. Calcium currents were also insignificant under our experimental conditions owing to the presence of 5 m*M* Co^{2+}, known to be very potent blocker of calcium channels (Brown et al. 1981; Carbone and Lux 1984). Holding potential was maintained at −90 mV. In all cases, the major part of the capacitive component of the membrane current in response to a voltage-step stimulation was compensated analogically. The full correction of capacitance and leak responses was made digitally online (see below).

Data acquisition

Stimulation and data acquisition were controlled by a microcomputer (Atari 1040ST), equipped with a 12 bit A/D-D/A converter (M2-Lab, Instrutech). Before digital acquisition at 50 kHz, currents were low-pass filtered by a 4-pole Bessel filter (Ithaco, 4302), at a cut-off frequency of 5 kHz or 10 kHz.

Standard pulse protocols were used to study macroscopic properties of sodium currents. The voltage dependence of sodium current activation and kinetics of activation and inactivation were examined using a series of voltage pulses to various depolarizing levels between −40 and 130 mV, preceded by a −100 mV prepulse lasting 5 ms. Double-pulse stimulations composed of a fixed test pulse preceded by a 40 ms conditional test pulse to various voltage levels, from −80 mV to −5 mV, allowed us to characterize the voltage dependence of steady-state sodium channel inactivation. All stimulations for sodium current measurements were followed by a similar pulse protocol in which pulse amplitudes were reduced to 1/4 and the holding potential was brought to −110 mV (P/4 procedure, Bezanilla and Armstrong 1977). The P/4 responses were used to subtract linear membrane responses.

Data analysis

Voltage-dependent properties of sodium currents were analysed in terms of the Hodgkin and Huxley model (Hodgkin and Huxley 1952). The peak sodium current I_p was estimated by fitting the experimental record in a short interval around the peak with a third order polynomial. Means of peak currents were obtained from between 4 and 26 patches at each ionic concentration. All the fitting procedures are based on the standard least-chi-square procedure (Press et al. 1989).

Results

Mg^{2+} blocking effect on the sodium channel is concentration and voltage dependent

Macroscopic sodium currents were recorded in the whole-cell configuration of the patch-clamp technique, from −40 to 130 mV with different $[Mg^{2+}]_i$. In order to compare results obtained from different cells, currents were scaled by membrane area, calculated from the compensation of the capacity transient of each cell (using the empirical relation: 1 pF/100 μm²). The scaled maximum inward peak current measured from 3–5 DIC cells is 0.26 ± 0.08 pA/μm² (mean ± SD, $n = 21$ and $Na_i^+/Na_o^+ = 15/110$). The membrane capacity is 2.2 ± 0.3 pF (mean ± SD, $n = 63$). Figure 1 shows families of sodium currents obtained with different $[Mg^{2+}]_i$. It illustrates that the blocking effect of Mg_i^{2+} on sodium current increases upon increasing $[Mg^{2+}]_i$.

Relations of peak current to test potential, $I_p - V_m$, obtained at $[Na^+]_i = 15$ m*M*, 0 m*M* and 7 m*M* Mg_i^{2+} are shown in Fig. 2A. Sodium peak currents appear to be reduced at applied $V_m > 0$ mV in the presence of Mg_i^{2+}. However, this reduction of sodium current becomes striking when V_m is higher than the sodium equilibrium potential. The blocking effect of 7 m*M* $[Mg^{2+}]_i$ is still clearly observed when the intracellular Na^+ concentration is raised to 30 m*M*, as is shown in Fig. 2B. Nevertheless, the reduction of I_p by Mg_i^{2+}, especially on the inward currents, diminished upon increasing $[Na^+]_i$.

In order to evaluate the blocking effect of Mg_i^{2+} under different experimental conditions, we normalized the peak current obtained in the presence of Mg_i^{2+} by that in the absence of Mg_i^{2+}. Normalized peak currents, I_n, obtained at 15 m*M* and 30 m*M* Na_i^+ are compared in Table 2. It is shown that the blocking effect of Mg_i^{2+} increases when the intracellular Mg^{2+} concentration is increased. However, the same $[Mg^{2+}]_i$ leads a lower

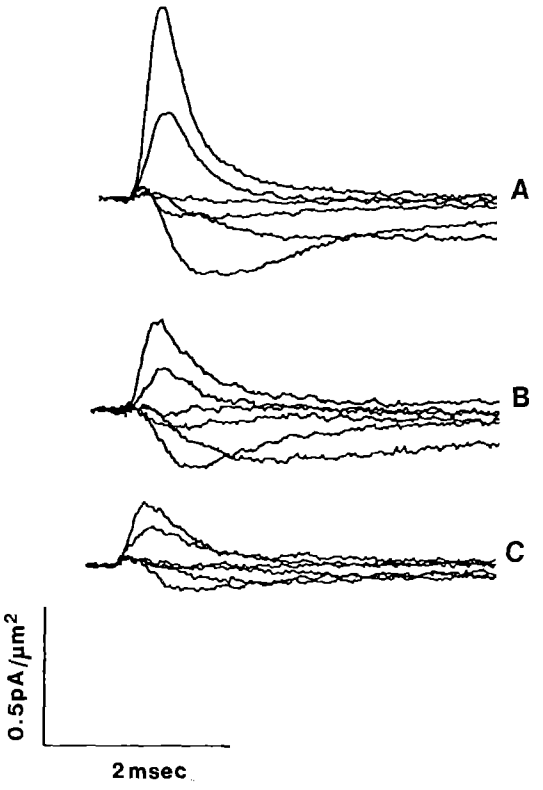

Fig. 1 A–C. Families of sodium currents obtained from three whole-cell patches. The holding potential was maintained at −90 mV. Voltage pulses to various test potentials from −20 to −80 mV in 20 mV steps, were preceded by a 5 ms prepulse of −100 mV. Each trace is the average of 8 records after the subtraction of linear leakage and capacitance currents. **A** was obtained with 0 m*M* $[Mg^{2+}]_i$, **B** with 0.5 m*M* $[Mg^{2+}]_i$ and **C** with 7 m*M* $[Mg^{2+}]_i$. All currents have been corrected by membrane areas. $[Na^+]_i = 15$ m*M* and $[Na^+]_o = 110$ m*M*

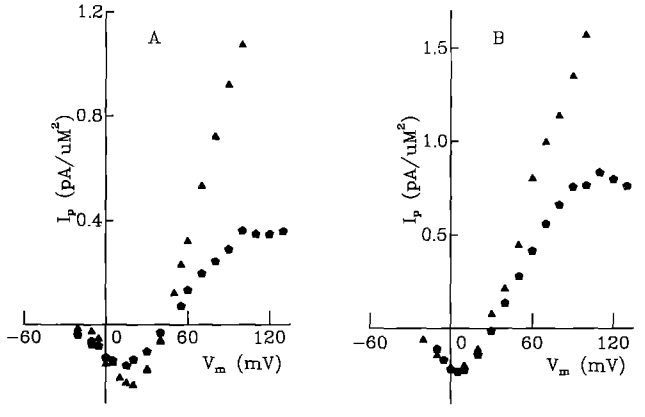

Fig. 2 A, B. Peak current (I_p)-membrane voltage (V_m) relationships. Triangles represent I_p obtained at $[Mg^{2+}]_i = 0$ m*M* and pentagons are values obtained at $[Mg^{2+}]_i = 7$ m*M*. Results were obtained from 4 different cells. **A** Peak currents were obtained at $[Na^+]_i = 15$ m*M*. Reversal potentials are 43.7 mV and 43.4 mV, in the presence of 0 and 7 m*M* Mg_i^{2+} respectively. **B** Peak currents were obtained at $[Na^+]_i = 30$ m*M*. Reversal potentials are 28.5 mV and 29.8 mV in the presence of 0 and 7 m*M* Mg_i^{2+}. All peak currents have been corrected by membrane areas. $[Na^+]_o = 110$ m*M* in both cases

Table 2. Normalized mean peak currents (I_n) obtained at an applied potential of 100 mV, and different $[Na^+]_i$ and $[Mg^{2+}]_i$. Values represent mean ±SD. $[Na^+]_o$ is fixed at 110 m*M*

$[Mg^{2+}]_i$	I_n ($[Na^+]_i = 15$ m*M*)	I_n ($[Na^+]_i = 30$ m*M*)
0.0	1.00±0.08 ($n=20$)	1.00±0.07 ($n=26$)
0.5	0.67±0.07 ($n=9$)	0.84±0.08 ($n=4$)
3.0	0.51±0.09 ($n=9$)	0.64±0.04 ($n=3$)
7.0	0.35±0.07 ($n=6$)	0.47±0.04 ($n=6$)

Table 3. Normalized mean peak currents (I_n) obtained at an applied potential of 100 mV, and different $[Na^+]_o$ and $[Mg^{2+}]_i$. Values represent mean±SD. $[Na^+]_i$ is fixed at 30 m*M*

$[Mg^{2+}]_i$	I_n ($[Na^+]_o = 50$ m*M*)	I_n ($[Na^+]_o = 70$ m*M*)	I_n ($[Na^+]_o = 110$ m*M*)
0.0	1.00±0.13 ($n=10$)	1.00±0.07 ($n=16$)	1.00±0.07 ($n=26$)
1.0	0.70±0.10 ($n=8$)	0.73±0.05 ($n=10$)	0.78±0.09 ($n=4$)
3.0	0.56±0.07 ($n=8$)	0.60±0.06 ($n=10$)	0.64±0.04 ($n=3$)
7.0	0.43±0.10 ($n=7$)	0.45±0.10 ($n=9$)	0.47±0.04 ($n=6$)

Table 4. The time to peak (ms), evaluated at different applied membrane potentials. Values are mean±SD. ($[Na^+]_i = 15$ m*M*, $[Na^+]_o = 110$ m*M*)

$[Mg^{2+}]_i$	10 mV	80 mV	100 mV	N
0.0	1.57±0.17	0.47±0.04	0.47±0.04	15
0.5	1.29±0.19	0.48±0.03	0.45±0.03	4
1.0	1.44±0.41	0.44±0.02	0.42±0.03	5
3.0	1.22±0.19	0.45±0.04	0.40±0.04	9
7.0	1.33±0.20	0.47±0.02	0.44±0.02	5

blocking effect with increasing $[Na^+]_i$. I_n, obtained in 50 m*M* and 110 m*M* Na_o^+ are compared in Table 3. Decreasing extracellular Na_o^+ concentration appears to slightly enhance the Mg_i^{2+} blocking effect. These observations suggest a competitive blocking mechanism of Mg^{2+} on the sodium channel. Hence, one can propose that Na^+ and Mg^{2+} competitively enter the sodium channel. The occupancy of the sodium channel by Mg^{2+}, therefore, interferes with the sodium flux in both directions.

Sodium channel gating mechanism is not significantly affected by Mg_i^{2+}

In order to investigate whether the reduction of sodium currents is an effect of Mg_i^{2+} on the gating mechanism of the sodium current we studied voltage-dependent gating parameters of sodium channels in the presence of different $[Mg^{2+}]_i$.

The first approach consisted of a comparison of voltage-dependent properties of peak currents in the presence of different $[Mg^{2+}]_i$. The time to peak, t_p, was estimated as an approximation of the activation time constant. The invariance of t_p measured at different applied potentials in the presence of $[Mg^{2+}]_i \leq 7$ m*M* is presented in Table 4.

Table 5. Half activation potential (V_h) and e-fold voltage dependence of activation (a). Data were obtained from fitting the peak current, estimated at each potential, with the equation: $I_p = g_{max}(V_m - V_{Na})/[1 - \exp((V_m - V_h)/a)]$ (Pröbstle et al. 1988). Values are mean ± SD. ($[Na^+]_i = 15$ mM, $[Na^+]_o = 110$ mM)

$[Mg^{2+}]_i$	V_h (mV)	a (mV)	N
0.0	10.8 ± 2.1	9.9 ± 0.9	13
0.5	10.5 ± 2.1	10.1 ± 1.3	6
1.0	9.2 ± 1.0	9.4 ± 1.2	6
3.0	11.8 ± 1.9	10.1 ± 1.0	5
7.0	10.4 ± 3.0	9.6 ± 1.2	11

Activation curves were constructed from I_p values obtained at different concentrations of Mg_i^{2+}. The half activation potential, V_h, and the e-fold dependence of I_p, a, were calculated according to Pröbstle and co-workers (1988). No significant changes of V_h and a were found when $[Mg^{2+}]_i \leq 7$ mM, as shown in Table 5.

A further and more precise analysis of the gating mechanism of sodium channels in the presence of Mg_i^{2+} was performed, using the Hodgkin-Huxley model (Hodgkin and Huxley 1952), as described by Moran and Conti (1990) and Lin and Moran (1990). In this case, sodium currents measured in the presence of different $[Mg^{2+}]_i$ were analysed.

With the addition of an empirical delay, δt, at the onset of the classical $m^3 h$ kinetics (Keynes and Royas 1974), sodium currents can be described as:

$$I(t) = I'\left(1 - \exp\left(-\frac{t-\delta t}{\tau_m}\right)\right)^3 \exp\left(-\frac{t-\delta t}{\tau_h}\right), \quad (1)$$

where, $I' = g_{max}(V_m - V_{ref})\, m_\infty^3\, h_0$. Fitting current traces obtained at each potential with Eq. (1) give directly the voltage dependence of activation and inactivation kinetics time constants, τ_m and τ_h, and that of the steady state activation parameter, m_∞. We have estimated τ_m and τ_h at different $[Mg^{2+}]_i$. It was found that both τ_h and τ_m are not significantly different at $[Mg^{2+}]_i \leq 7$ mM. However, the voltage-dependence of τ_m and τ_h do significantly shift about −25 mV when $[Mg^{2+}]_i$ is changed from 0 to 30 mM, as shown in Fig. 3A and B.

The voltage dependence of the steady-state activation parameter, m_∞, is characterized by the half-activation potential, $V_{1/2}^m$, at which the open-state probability for each activation gate is 0.5, and by the apparent valence z_m of a single activation process (m-gate). These parameters were obtained by a least-squares fit to the equation

$$m_\infty(V_m) = \frac{1}{1 + \exp\left(z_m e_0 \frac{V_{1/2}^m - V_m}{k_b T}\right)}, \quad (2)$$

where, e_0 is the proton charge (1.6×10^{-19} Coulomb), k_B is the Boltzmann constant and T is the absolute temperature.

The voltage dependence of the steady state inactivation parameter, h_∞, was obtained by fitting the peak current, obtained from traditional double-pulse experiments, against the prepulse potential:

$$h_\infty \simeq \frac{I_p}{I_p^{max}} = \frac{1}{1 + \exp\left(\frac{V_{pp} - V_{1/2}^m}{a_h}\right)}, \quad (3)$$

where, $V_{1/2}^m$ and a_h characterize the half-inactivation potential and the steepness of the voltage-dependence. I_p^{max} is the maximum peak current measured and V_{pp} is the prepulse potential.

Activation and inactivation parameters, estimated with different $[Mg^{2+}]_i$, are compared in Table 6. Values of $V_{1/2}^m$ and $V_{1/2}^h$ indicate no significant difference at $[Mg^{2+}]_i \leq 7$ mM. However, both $V_{1/2}^m$ and $V_{1/2}^h$ show significant negative shifts, which are in the range −25 to −29 mV, when $[Mg^{2+}]_i$ was increased from 0 to 30 mM. The voltage dependence of activation and inactivation processes, expressed as z_m and a_h, do not show any significant change when $[Mg^{2+}]_i$ is increased from 0 up to 30 mM. The voltage dependence of m_∞ and h_∞, in the presence of 0 and 30 mM Mg_i^{2+}, are compared in Fig. 3C and D.

These results suggest that the effect of Mg_i^{2+} on sodium gating processes is non-linearly dependent on its concentration. There is a similar shift in the range −25 to −29 mV in the activation and inactivation processes. Nevertheless, the steepness of the voltage dependence of the gating processes, as revealed by the analysis of activation and inactivation curves, was not affected by 30 mM Mg_i^{2+}. This is consistent with a local surface potential change produced by Mg^{2+} on the intracellular membrane surface. Similar interpretations have been proposed by Hille (1968) and Hahin and Campbell (1983) to explain the effect of extracellular Ca^{2+} on sodium currents.

Kinetic model of the Mg_i^{2+} blocking mechanism

In order to account for the dependence of the Mg_i^{2+} blockage on Na_i^+ and Na_o^+, we investigated a simple permeation model based on Michaelis-Menten reaction kinetics in enzymatic reactions.

Permeation of Na^+ through the sodium channel can be described as a binding process, i.e. Na^+ has to bind to sites inside the channel during its passage through the membrane, and one site can bind only one ion at a time. The sodium flux depends on the rate constants of the Na^+ binding and dissociation processes. The sodium permeation process can be described by the following scheme:

$$S + Na_i^+ \underset{k_{-1}}{\overset{k_1[Na^+]_i}{\rightleftharpoons}} SNa^+ \underset{k_{-2}[Na^+]_o}{\overset{k_2}{\rightleftharpoons}} S + Na_o^+$$

Although there may be more than one binding site inside the sodium channel (Hille 1975; Begenisich and Cahalan 1980a, b), we will use the one-binding site model to describe the sodium flux in order to simplify quantitative calculations, based on the assumption that the flux is mainly determined by the rate constants for Na^+ with its rate-limiting site. Therefore, in the sodium permeation

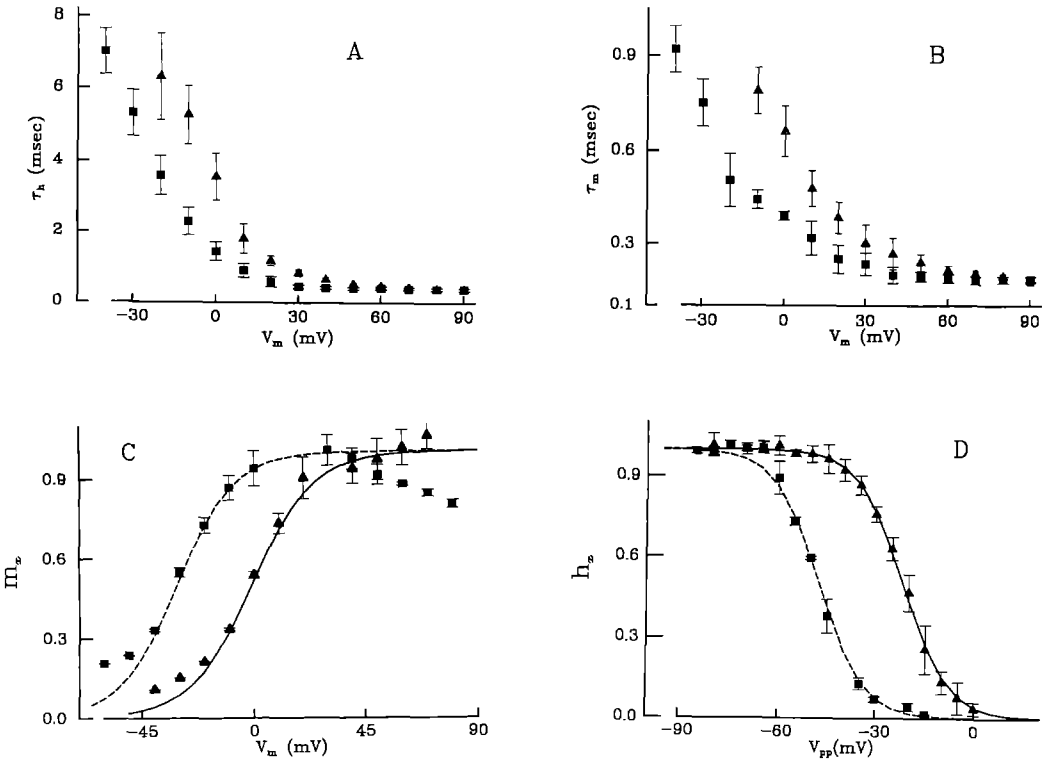

Fig. 3A–D. The voltage dependence of gating parameters of sodium channels. *Triangles* are values measured in the absence of Mg_i^{2+}, *squares* are those with $[Mg^{2+}]_i = 30$ m*M*. $[Na^+]_i = 30$ m*M*, $[Na^+]_o = 110$ m*M* in all experiments. Voltage-dependent inactivation (**A**) and activation (**B**) time constants. Each *point* represents the mean of measurements made from at least 8 different cells. *Bars* represent their standard deviations. Voltage shifts in both cases are about −25 mV, when $[Mg^{2+}]_i$ is increased from 0 to 30 m*M*. Time constants measured in the presence of 7 m*M* Mg_i^{2+} (not shown) overlay quite well with those obtained at 0 m*M* Mg_i^{2+}. **C** Steady state activation parameter m_∞ of sodium currents is shown as a function of test potential. Data points are mean values obtained from seven patches with 0 m*M* Mg_i^{2+} and six patches with 30 m*M* Mg_i^{2+}. *Bars* represent their standard deviations. Smooth lines were obtained by fitting data with (2). $V_{1/2}^m$ shifts is -29.1 ± 0.4 mV. (**D**) Voltage dependence of steady state inactivation parameter h_∞ of sodium currents. Normalized peak inward current responses to the test pulse are plotted as a function of the prepulse potential as described in the text. Data points represent means obtained from five patches with 0 m*M* Mg_i^{2+} and four patches with 30 m*M* Mg_i^{2+}. Smooth lines are the least-square fitting data to (3). $V_{1/2}^I$ shift is -25.7 ± 7.8 mV

Table 6. Activation ($V_{1/2}^m$, z_m) and inactivation ($V_{1/2}^h$, a_h) parameters, which characterize the voltage dependence of steady state activation and inactivation parameters of the Hodgkin-Huxley model. ($[Na^+]_i = 30$ m*M* $[Na^+]_o = 110$ m*M*)

$[Mg^{2+}]_i$	$V_{1/2}^m$ (mV)	z_m	N	$V_{1/2}^h$ (mV)	a_h (mV)	N
0.0	-1.8 ± 0.1	2.1 ± 0.2	7	-21.8 ± 3.9	-6.9 ± 0.6	5
0.5				−19.2	−6.1	1
1.0	-6.5 ± 4.3	2.0 ± 0.4	3	−26.9	−6.7	1
3.0	−1.4	1.9	1			
7.0	-4.3 ± 3.1	2.0 ± 0.2	5	-26.6 ± 4.5	-6.8 ± 2.2	2
30.0	-30.9 ± 0.1	2.2 ± 0.2	6	-47.5 ± 3.9	-6.9 ± 0.3	4

scheme above, *S* represents the sodium channel, SNa^+ is the binding state of Na^+, *k*'s represent rate constants of Na^+ reactions in different directions. All of the rate constants are functions of membrane potential and depend on the chemical potential associated with their relative reactions. The binding of Na^+ with its rate-limiting sites can be directly described by voltage-dependent Michaelis constants K_{Na_i} and K_{Na_o}, which are defined as: $K_{Na_i}(V_m) = (k_{-1} + k_2)/k_1$ for Na_i^+ and $K_{Na_o}(V_m) = (k_{-1} + k_2)/k_{-2}$ for Na_o^+. In the presence of a competitive blocker, Mg_i^{2+}, the permeation through sodium channels described above may be modified as:

$$S + Na_i^+ \underset{k_{-1}}{\overset{k_1[Na^+]_i}{\rightleftharpoons}} SNa^+ \underset{k_{-2}[Na^+]_o}{\overset{k_2}{\rightleftharpoons}} S + Na_o^+$$

$$+ \quad Mg_i^{2+}$$

$$k_{-3} \uparrow\downarrow k_3[Mg^{2+}]_i$$

$$SMg^{2+} \qquad ** \text{ Blocked state}$$

where SMg^{2+} represents Mg_i^{2+} bound to the sodium channel S. Because no magnesium ion exists on the extracellular side of the membrane, binding of Mg^{2+} to the sodium channel can be directly characterized by a voltage-dependent dissociation constant $K_{Mg}(V_m)$, defined as $K_{Mg}(V_m)=k_{-3}/k_3$.

Therefore, the sodium flux in the presence of Mg_i^{2+} is described as:

$$I(t, V_m, [Na^+]_i, [Na^+]_o, [Mg^{2+}]_i) = \frac{\bar{I}(t, V_m, [Na^+]_i, [Na^+]_o, 0)(1+A)}{1+\left(1+\frac{[Mg^{2+}]_i}{K_{Mg}(V_m)}\right)A} \quad (4)$$

where, $A \equiv 1/(K_{Na_i}(V_m)/[Na^+]_i + K_{Na_o}(V_m)/[Na^+]_o)$. I is the sodium current directly measured in the presence of Mg_i^{2+}. It is a function of time, t, membrane potential, V_m, and $[Na^+]_i$, $[Na^+]_o$, $[Mg^{2+}]_i$. $\bar{I}$ is the current measured in the absence of Mg_i^{2+}. In order to supersede the time variable, the peak sodium current I_p was applied in our analysis.

$$I_p(V_m, [Na^+]_i, [Na^+]_o, [Mg^{2+}]_i) = I'_p(V_m, [Na^+]_i, [Na^+]_o, [Mg^{2+}]_i) \cdot P_0(V_m, [Na^+]_i, [Na^+]_o, [Mg^{2+}]_i), \quad (5)$$

where I_p is the peak current which can be measured directly at applied membrane potential V_m, I'_p is the theoretical peak current when all sodium channels are in conductive states and P_0 is the probability of a channel being in a conductive state. Normalizing peak current (I_n) as:

$$I_n(V_m, [Na^+]_i, [Na^+]_o, [Mg^{2+}]_i) = I_p(V_m, [Na^+]_i, [Na^+]_o, [Mg^{2+}]_i)/ I_p(V_m, [Na^+]_i, [Na^+]_o, 0),$$

Equation (4) can be simplified to:

$$I_n(V_m, [Na^+]_i, [Na^+]_o, [Mg^{2+}]_i) = \frac{1}{1+\frac{[Mg^{2+}]_i}{K_{Mg}^{app}(V_m, [Na^+]_i, [Na^+]_o)}}, \quad (6)$$

where the apparent binding constant K_{Mg}^{app} is defined as:

$$K_{Mg}^{app}(V_m, [Na^+]_i, [Na^+]_o) = K_{Mg}(V_m)\left(1+\frac{[Na^+]_i}{K_{Na_i}(V_m)}+\frac{[Na^+]_o}{K_{Na_o}(V_m)}\right). \quad (7)$$

It is noteworthy that the peak current analysis method, proposed above, can be applied only if the gating mechanism of the sodium channel is not significantly influenced by Mg_i^{2+}, i.e. P_0 in Eq. (5) is not signficantly influenced by the presence of Mg_i^{2+}. This condition is satisfied when $[Mg^{2+}]_i \leq 7$ mM, which has been demonstrated in the previous section (see also Tables 4, 5 and 6). If this is the case I_n would be expected to approach a constant, at least in a range where I'_p is not significantly influenced by Mg_i^{2+}. Figure 4 illustrates this behavior of I_n. It shows that I_n is quite constant at potentials lower than the sodium equilibrium potential, which is around 31 mV with 0 or 7 mM Mg_i^{2+}, and decreases in a voltage-dependent way when the potential increases.

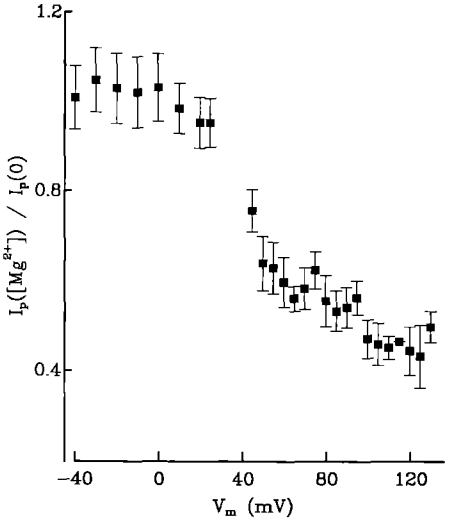

Fig. 4. Normalized sodium peak currents I_n evaluated at different membrane potentials V_m. Data points I_n were obtained by normalizing $I_p([Mg_i^{2+}])$ obtained with 7 mM Mg_i^{2+} by I_p obtained in the absence of Mg_i^{2+}. *Bars* represent their standard deviations after such normalization. Normalized data points were from 23 control patches and 8 Mg_i^{2+} patches. Sodium equilibrium potentials are 30.8 ± 2.7 mV (0 mM Mg_i^{2+}) and 31.3 ± 3.7 mV (7 mM Mg_i^{2+}). $[Na^+]_i = 30$ mM and $[Na^+]_o = 110$ mM. I_n fluctuates around 1 when membrane potential is lower than the sodium equilibrium potential, which suggests there is no significant influence of Mg_i^{2+} on the gating mechanism of the sodium channel. The decrease of I_n at membrane potentials higher than the sodium equilibrium potential indicates the voltage-dependent blockage of sodium currents by Mg_i^{2+}

K_{Mg}^{app} has been calculated from I_n at different membrane potentials V_m and different ionic concentrations, $[Na^+]_i$ and $[Na^+]_o$, according to Eq. (6). Its dependence on V_m, $[Na^+]_i$ and $[Na^+]_o$ is illustrated in Fig. 5. The dissociation constant $K_{Mg}(V_m)$, Michaelis constants $K_{Na_i}(V_m)$ and $K_{Na_o}(V_m)$ are further obtained by fitting K_{Mg}^{app} against $[Na^+]_i$ and $[Na^+]_o$, using Eq. (7). Results are represented as data points in Fig. 6.

In the Appendix we show that the voltage-dependent dissociation constant $K_{Mg}(V_m)$ of Mg_i^{2+} for the sodium channel, as well as Michaelis constants for Na^+: $K_{Na_i}(V_m)$ and $K_{Na_o}(V_m)$, can be further expressed in term of the free energy of the ionic binding-dissociation process. They are given as:

$$K_{Mg}(V_m) = K_{Mg}(0)\exp(-2BV_m\delta') \quad (8)$$

$$K_{Na_i}(V_m) = K_i(0)\exp(-BV_m\delta) + K'_i\exp\left(\frac{BV_m}{2}\right)\exp(-BV_m\delta) \quad (9)$$

$$K_{Na_o}(V_m) = K_0(0)\exp(BV_m(1-\delta)) + K'_0\exp\left(-\frac{BV_m}{2}\right)\exp(BV_m(1-\delta)), \quad (10)$$

where, B is defined as F/RT. F is the Faraday constant and R the ideal gas constant. δ' and δ represent the fraction of total electrical potential drop, between the inside

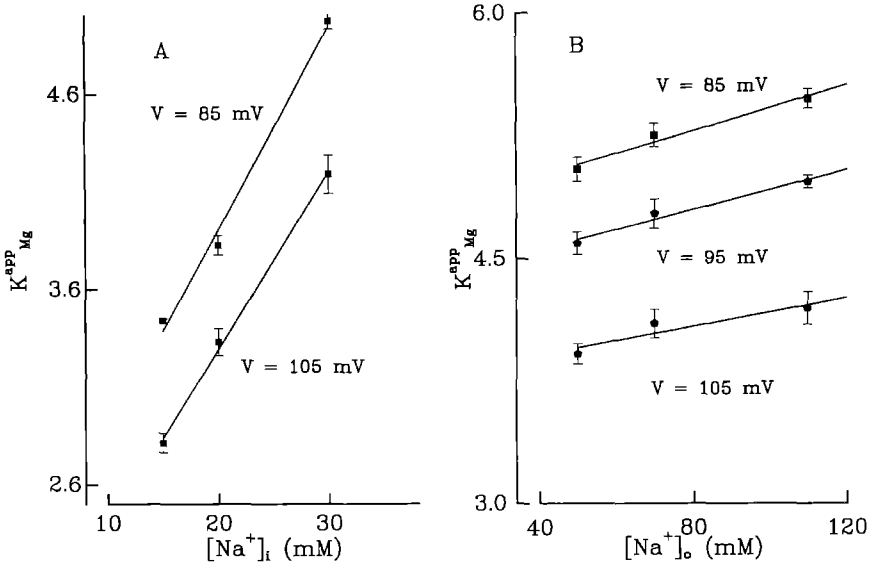

Fig. 5A, B. Apparent binding constant K_{Mg}^{app} as a function of $[Na^+]_i$ (**A**) and $[Na^+]_o$ (**B**). K_{Mg}^{app} were obtained from Eq. (6), at different membrane potentials V_m and different ionic concentrations $[Na^+]_i$ and $[Na^+]_o$. K_{Mg}^{app} were plotted as data points in figures, *bars* represent their standard deviations. K_{Mg}^{app} were further fitted with Eq. (7) against $[Na^+]_i$ with $[Na^+]_o$ fixed at 10 m*M* (**A**), or against $[Na^+]_o$ with $[Na^+]_i$ fixed at 30 m*M* (**B**). Fitting results are represented as smooth lines in figures

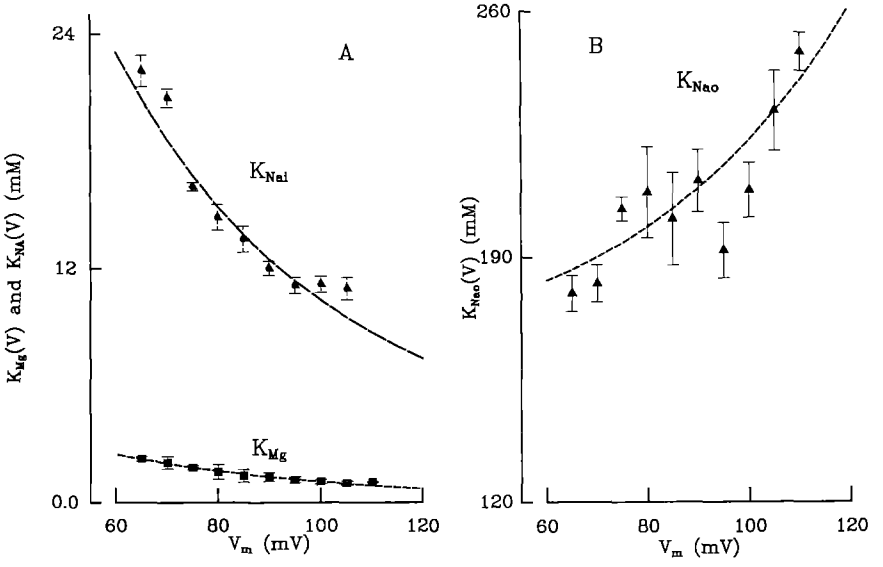

Fig. 6A, B. The voltage dependence of dissociation constants $K_{Mg}(V_m)$ (*squares*) and Michaelis constants $K_{Na_i}(V_m)$ (*triangles*) are illustrated in **A**. The voltage dependence of Michaelis constant $K_{Na_o}(V_m)$ is shown in **B**. Each data point was obtained by fitting K_{Mg}^{app} (V_m, $[Na^+]_i$, $[Na^+]_o$) as a function of $[Na^+]_i$ and $[Na^+]_o$ respectively, using Eq. (7). *Bars* are standard deviations obtained from calculations. Smooth lines were obtained by fitting $K_{Mg}(V_m)$ to Eq. (8) and $K_{Na_i}(V_m)$, $K_{Na_o}(V_m)$ to Eqs. (9) and (10). Fitting results are detailed in the text

surface of the membrane and the Mg^{2+} and Na^+ binding sites respectively (in this text, it will be called the electrical distance from the inside). $K_{Mg}(0)$ is the dissociation constant of Mg^{2+} for the sodium channel at zero membrane potential. $K_{Mg}(0) = \varrho^{-1} \exp(-\delta G_{Mg}/(k_B T))$. Fixing the zero reaction free energy level at $\varrho = 1$, which corresponds to $K_{Mg}(0) = 1\ M$, i.e. the equilibrium state, the free energy of the Mg^{2+} binding dissociation reaction, δG_{Mg}, can be expressed as:

$$\delta G_{Mg} = -k_B T \ln (K_{Mg}(0)) \tag{11}$$

$K_i(0) \equiv k_{-1}/k_1$ and $K_o(0) \equiv k_2/k_{-2}$ are dissociation constants of Na_i^+ and Na_o^+ for the sodium channel at zero membrane potential. Relations between $K_i(0)$ and $K_o(0)$ and the reaction free energy are similar to Eq. (11). K_i' and K_o' represent the outward and inward sodium flux probability (see Appendix).

Values of $K_{Mg}(V_m)$, $K_{Na_i}(V_m)$ and $K_{Na_o}(V_m)$, obtained from Eq. (7) have been further fitted with Eqs. (8), (9) and (10) respectively. Results are shown as smooth lines in Fig. 6. From these fittings, dissociation constants of Mg^{2+}, Na_i^+ and Na_o^+ with their binding sites inside the sodium channel at $V_m = 0$ mV have been estimated. For Mg^{2+}, $K_{Mg}(0)$ was estimated to be 8.65 ± 1.51 m*M*, which corresponds to a reaction free energy of $4.75 \pm 0.17\ k_B T$. The location of the Mg^{2+} binding site inside the sodium channel is 0.26 ± 0.03 electrical distance from the inner membrane surface. The zero membrane potential dissociation constant for Na_i^+, $K_i(0)$, is estimated to be 83.76 ± 7.60 m*M*, corresponding to $\delta G = 2.48 \pm 0.09\ k_B T$, which is smaller than that of Mg^{2+}. The location of the Na_i^+ binding site is at 0.75 ± 0.23 electrical distance from inner membrane surface. Finally, for extracellular Na^+, the dissociation constant $K_o(0)$ is 20.86 ± 1.49 m*M* with $\delta = 0.58 \pm 0.05$ electrical distance from the inner membrane surface. The free energy of the Na_o^+ binding-dissociation process is calculated to be $3.87 \pm 0.07\ k_B T$ unit, which is smaller than that for Na_i^+. This difference be-

tween Na_i^+ and Na_o^+ reaction free energies reflects that chemical potential differences exist between Na^+ on the both sides of the membrane. This difference should lead to different favourable reaction directions for Na_i^+ and Na_o^+.

Discussion

The blockage of sodium current by intracellular Mg^{2+} already described by Pusch et al. (1989) and Pusch (1990) has been used to explain the observed reduction of outward Na^+ current as a deviation from the Goldman-Hodgkin-Katz equation. The aim of this work was to investigate if this blockage also occurs in neural cells, and if it is possible to describe it in more molecular terms, based on a kinetic model.

In order to investigate if Mg_i^{2+} influences the voltage-dependent gating process of the sodium channel we analysed sodium currents in terms of the Hodgkin-Huxley model. We found no significant influence on gating parameters at $[Mg^{2+}]_i \leq 7$ mM. Nevertheless, all steady-state and kinetic gating parameters show a similar shift in the range -25 mV to -29 mV when $[Mg^{2+}]_i$ is increased from 0 to 30 mM, while the steepness of voltage-dependence of activation and inactivation are not affected. These equal shifts could be explained as a change of intracellular surface potential caused by Mg_i^{2+}, which screens negative charges on the inner surface and changes the local electrical field. From these findings, we concluded that the modification of the gating mechanism may enforce the reduction of sodium currents, but it is insufficient to explain Mg^{2+} blocking behaviour which is voltage-, $[Mg^{2+}]_i$-, $[Na^+]_i$- and $[Na^+]_o$-dependent.

We have proposed a model in which Na^+ and Mg^{2+} competitively occupy the sodium channel. In this model, Na^+ and Mg^{2+} have to bind to the sodium channel during their passage through the membrane. The blockage of sodium currents may be caused by Mg^{2+} occupying the sodium channel, which prevents the further binding of Na^+ (if the binding site for Mg^{2+} is one of binding sites for Na^+ during its passage) or interferes with the normal accommodation of Na^+ by sodium channels. The sodium permeation in the presence of the competitive blocker Mg_i^{2+} has, therefore, been described as a voltage-dependent binding-unbinding process, based on Michaelis-Menten reaction kinetics. The normalized peak sodium current, I_n, has been introduced to describe quantitatively the Mg_i^{2+} blockage model, with the condition that there is no significant influence of Mg^{2+} on the gating mechanism of sodium currents. Using this simple model we can explain the Mg^{2+} blockage quite well. Furthermore, the model also provides a simple way to calculate the voltage dependence of the dissociation constant of Mg^{2+} with site S, as well as Michaelis constants for intracellular and extracellular Na^+ with this site (Fig. 6). The former directly illustrates the blocking capability of Mg^{2+}. The latter two constants illustrate the influence of Na^+ from different sides on the binding site as functions of membrane potential, as well as the interdependence between Na_i^+ and Na_o^+ in the sodium permeation.

Relations between the dissociation constant $K_{Mg}(V_m)$, Michaelis constants $K_{Na_i}(V_m)$, $K_{Na_o}(V_m)$ and membrane potential V_m have been further described in terms of the reaction free energy, with additive Eyring rate factors to account for the effect of the applied electrical field (see Appendix). With these relations, it provides a way to locate the binding site of Na^+ and Mg^{2+} in the sodium channel. It was found that the rate-limiting binding site of Na_0^+ and Na_i^+ appears to be the same, it is located in the range of 0.58 ± 0.05 to 0.75 ± 0.23 electrical distance from the inner membrane surface. This location of the Na^+ binding site, δ, is in agreement with those calculated by others: $1-\delta = 0.36$ for guinea pig heart sodium channel (Nilius 1988), $1-\delta = 0.37 \pm 0.2$ for neuroblastoma (Yamamoto et al. 1984). Nevertheless, the rate-limiting binding site of Mg^{2+} with the sodium channel appears to be different from that of Na^+, since $\delta' = 0.26 \pm 0.03$. This difference supports the argument that there may be more than one binding site inside the membrane (Hille 1975; Begenisich and Cahalan 1980a, b). However, independent of how many binding sites are necessary to accurately describe the sodium current, which would lead to different transient states of Na^+, i.e. NaS_1, NaS_2 etc., in the sodium permeation scheme, the kinetic model of Mg_i^{2+} blockage we proposed is still efficient, since one binding site can bind only one ion at a time. Mg^{2+} is probably not permeable but prevents Na^+ permeation by competitive binding to a site located at an electrical distance of 0.26 ± 0.03 from the internal surface of the membrane.

With voltage dependent relations of dissociation constants $K_{Mg}(V_m)$ and Michaelis constants $K_{Na_i}(V_m)$ and $K_{Na_o}(V_m)$, dissociation constants of Mg^{2+} and Na^+ for the sodium channel at zero membrane potential, $K_{Mg_o}(0)$, $K_i(0)$ and $K_0(0)$ have been calculated. The value of $K_{Mg}(0)$ is much smaller than that of $K_i(0)$, which reflects the high affinity of Mg^{2+} for the sodium channel. In fact, the reaction free energies of both reactions calculated reflect the fact that the dissociation of Mg^{2+} from the sodium channel is less energy-favorable than that of Na_i^+, since $\delta G_{Mg} = 4.75 \pm 0.17$ and $\delta G_i = 2.48 \pm 0.09\ k_B T$. Dissociation constants of Na_i^+ and Na_o^+ also appear to be different, which reflect the reaction free energy differences of Na_i^+ and Na_o^+, which leads to the different effect on sodium permeation by Na_i^+ and Na_o^+.

The blocking of the sodium channel by Mg^{2+} may be due to two different reasons. The first possibility is related to the selectivity of sodium channels. Mg^{2+} enters the sodium channel and binds to an inside site during membrane depolarization. Because of the selectivity of the pore (the permeability ratio of Mg^{2+} to Na^+ through the sodium channel is less than 0.1 (Hille 1972)), Mg^{2+} is not further permeable and is even kicked back due to the small extracellular Na^+ inward flux through the channel. The other possibility is that the strong binding force between Mg^{2+} and the site retards the release of Mg^{2+} from the channel. In fact, the dissociation constant value for Mg^{2+} binding within the sodium channel at zero membrane potential, is 8.65 ± 1.51 mM, which is much smaller than that for Na_i^+: $K_i(0) = 83.76 \pm 7.60$ mM. Most probably, these two possibilities may coexist and influence each other, which may lead to the entrance of Mg^{2+} into the

channel several times during the depolarization, giving a high frequency of flickering at the single channel level and thus produce an apparent single channel conductance decrease. This phenomenon has been observed in single channel measurements of a mutant sodium channel expressed in *Xenopus* oocytes (Pusch 1990). However, before choosing between these hypotheses, more experiments on the microscopic properties of the wild-type sodium channel, either in cells or expressed in oocytes, are needed.

The data presented here have shown that sodium currents of rat cerebellar granule cells can be blocked by intracellular magnesium in a voltage- and concentration-dependent manner, by Na^+ and Mg^{2+} competitively occupying the sodium channel. In a summary, we could get some general information from our analysis: (1) The affinity of Mg^{2+} for sodium channels is much higher than those of Na_i^+ and Na_o^+. At zero membrane potential, ionic affinities with sodium channels satisfy the relation $Na_i^+ < Na_o^+ < Mg_i^{2+}$. (2) The entrance of Mg^{2+} into the channel may be blocked at a site very close to the intracellular membrane surface. This location differs from that of the Na^+ rate-limiting binding site.

From our results, the half blocking concentration of Mg_i^{2+} is shown to be a decreasing function of applied membrane potential: K_{Mg} is 8.65 ± 1.51 mM at 0 mV; 1.37 ± 0.33 mM at 85 mV and 0.99 ± 0.10 mM at 105 mV. Dissociation constants obtained at high membrane potentials are comparable with the physiological intracellular Mg^{2+} concentration, which should be in the order of 1.7 mM, as measured in frog skeletal muscle (Alvarez-Leefmans et al. 1986). Our data suggest that the physiological Mg_i^{2+} concentration is sufficient to block sodium channels significantly when cells are exposed to considerable depolarization. This effect may correspond to a physiological regulation mechanism of sodium channels.

Appendix

The free energy of the reaction

A general process for the ionic binding-dissociation reaction, as indicated in our kinetic scheme for sodium permeation, can be described in terms of tunneling through barriers and wells. The corresponding partition function is the sum over all possible configurations of the reaction with appropriate Boltzmann factors. In terms of path-integral formalism, the partition function is given by

$$\Xi = \frac{1}{N} \int \mathscr{D}\phi \exp\left(-\frac{G[\phi]}{k_B T}\right), \tag{A-1}$$

where, ϕ is a general configuration of the reaction, $G[\phi]$ is the free energy function, k_B is the Boltzmann constant, T is the absolute temperature and N is a normalization factor.

For the Mg_i^{2+} dissociation reaction, the dissociation rate constant, k_{-3}, can be expressed as

$$k_{-3} = \int \mathscr{D}\phi \, 2\pi\omega[\phi] \exp\left(-\frac{G[\phi]}{k_B T}\right) \tag{A-2}$$

in which, $2\pi\omega[\phi]$ is the reaction rate for a given configuration ϕ. In the case of heavy ions, e.g. Mg^{2+} and Na^+, fluctuation effects can be ignored and a saddle point approximation is valid. In this approximation, we have

$$k_{-3} = 2\pi\omega_{-3} \exp\left(-\frac{G_{Mg}^-}{k_B T}\right) \tag{A-3-a}$$

where, G_{Mg}^- is the free energy associated with the most probable configuration of the dissociation reaction, and $2\pi\omega_{-3}$ is the corresponding reaction rate which can be further expressed in terms of the thermal energy $k_B T$, i.e. $2\pi\omega_{-3} = k_B T/h$, where h is the Planck constant.

Analogously, the rate constant of the Mg^{2+} binding process can be expressed as

$$k_3 = \varrho \frac{k_B T}{h} \exp\left(-\frac{G_{Mg}^+}{k_B T}\right) \tag{A-3-b}$$

where G_{Mg}^+ is the free energy of the binding reaction. ϱ is a constant with the dimension of M^{-1}, to be fixed by the zero-free energy level of the reaction.

Similarly, binding and dissociation rate constants for Na_i^+ and Na_o^+ are expressed as

$$k_1 = \varrho_i \frac{k_B T}{h} \exp\left(-\frac{G_i^+}{k_B T}\right) \tag{A-3-c}$$

$$k_{-1} = \frac{k_B T}{h} \exp\left(-\frac{G_i^-}{k_B T}\right) \tag{A-3-d}$$

$$k_{-2} = \varrho_o \frac{k_B T}{h} \exp\left(-\frac{G_o^+}{k_B T}\right) \tag{A-3-e}$$

$$k_2 = \frac{k_B T}{h} \exp\left(-\frac{G_o^-}{k_B T}\right) \tag{A-3-f}$$

in which, subscripts of G, 'i' and 'o' refer to reactions of Na_i^+ and Na_o^+ respectively. '+' and '−' refer the binding and dissociation processes. ϱ_i and ϱ_o are constants fixed by zero-free energy levels for reactions of Na_i^+ and Na_o^+.

In the presence of an applied membrane potential V_m, additional Eyring rate factors (Eyring 1935) have to be included in equations (A-3), in order to take into account the electrical field effect introduced. Therefore, the dissociation constant of Mg^{2+} is:

$$K_{Mg}(V_m) \equiv \frac{k_{-3}}{k_3} = K_{Mg}(0) \exp(-2BV_m\delta'). \tag{A-4}$$

Analogously, voltage-dependent Michaelis constants, $K_{Na_i}(V_m)$ and $K_{Na_o}(V_m)$, are expressed as:

$$K_{Na_i}(V_m) \equiv \frac{k_{-1}+k_1}{k_1} = K_i(0) \exp(-BV_m\delta) + K_i' \exp\left(\frac{BV_m}{2}\right) \exp(-BV_m\delta) \tag{A-4}$$

$$K_{Na_o}(V_m) \equiv \frac{k_{-1}+k_1}{k_1} = K_o(0) \exp(BV_m(1-\delta)) + K_o' \exp\left(-\frac{BV_m}{2}\right) \exp(BV_m(1-\delta)) \tag{A-5}$$

in which, B is defined as F/RT. δ' and δ represent the fraction of total electrical potential drop, between the inside surface of the membrane and the Mg^{2+} and Na^+

binding sites respectively (the total electrical potential drop across the membrane is assumed to be 1).

$$K_i' \equiv \frac{1}{\varrho_i} \exp\left(-\frac{G_o^- - G_i^+}{k_B T}\right)$$

and

$$K_o' \equiv \frac{1}{\varrho_o} \exp\left(-\frac{G_i^- - G_o^+}{k_B T}\right).$$

$K_{Mg}(0)$, $K_i(0)$ and $K_o(0)$ are the dissociation constants of Mg^{2+}, Na_i^+ and Na_o^+ for the sodium channel at zero membrane potential. They are defined as

$$K_{Mg}(0) = \frac{1}{\varrho} \exp -\left(\frac{\delta G_{Mg}}{k_B T}\right),$$

$$K_i(0) = \frac{1}{\varrho_i} \exp -\left(\frac{\delta G_i}{k_B T}\right)$$

and

$$K_o(0) = \frac{1}{\varrho_o} \exp -\left(\frac{\delta G_o}{k_B T}\right)$$

where δG represents different ionic binding-dissociation reaction free energies at zero membrane potential, with subscripts related to Mg^{2+}, Na_i^+ and Na_o^+.

Fixing the zero-free energy level at $\varrho = 1$, which corresponds to dissociation constants of $1\,M$, i.e. fixing the zero-free energy levels at equilibrium states at $V = 0$ mV, free energies of reactions of Mg^{2+}, Na_i^+ and Na_o^+ systems can be calculated as:

$$\delta G_{Mg} = -k_B T \ln K_{Mg}(0) \quad \text{(A-7)}$$

$$\delta G_i = -k_B T \ln K_i(0) \quad \text{(A-8)}$$

$$\delta G_o = -k_B T \ln K_o(0) \quad \text{(A-9)}$$

References

Altura BM, Altura BT (1985) New perspectives on the role of magnesium in the patho-pyhsiology of the cardiovascular system. Magnesium 4:245–271

Alvarez-Leefmans FJ, Gamino SM, Giraldez F, Gonzales-Serratos H (1986) Intracellular free magnesium in frog skeletal muscle fibers measured with ion-selective micro-electrodes. J Physiol (London) 378:461–483

Baker PF, Dipolo R (1984) Axonal calcium and magnesium homeostasis. In: Baker PF (ed) Current topics in membrane and transport: The squid axon, vol 22. Academic Press, New York, pp 195–247

Begenisich TB, Cahalan MD (1980a) Sodium channel permeation in squid axon I: reversal potential measurements. J Physiol (London) 307:217–242

Begenisich TB, Cahalan MD (1980b) Sodium channel permeation in squid axon II: non-independence and current-voltage relations. J Physiol (London) 307:243–257

Bezanilla F, Armstrong M (1977) Inactivation of sodium channel. II Gating current experiments. J Gen Physiol 70:549–566

Brown AM, Murimoto K, Tsua Y, Wilson DL (1981) Calcium current-dependent and voltage-dependent inactivation of calcium channel in *Helix aspersa*. J Physiol (London) 320:193–218

Carbone E, Lux HD (1984) A low voltage activated, fully inactivated Ca channel in sensory neurons. Nature 310:501–502

Cull-Candy SG, Marshall CG, Ogden D (1989) Voltage-dependent membrane currents in rat cerebellar neurones. J Physiol (London) 414:179–199

Eyring H (1935) The activated complex in chemical reactions. J Chem Phys 3:107–115

Hahin R, Campbell DT (1983) Simple shifts in the voltage dependence of sodium channel gating caused by divalent cations. J Gen Physiol 82:785–802

Hamill OP, Marty A, Neher E, Sakmann B, Sigworth FJ (1981) Improved patch-clamp techniques for high resolution current recording from cells and cell-free membrane patches. Pflügers Arch 391:85–100

Hille B (1968) Charges and potentials at the nerve surface: Divalent ions and pH. J Gen Physiol 51:199–219

Hille B (1972) The permeability of sodium channel to metal cations in myelinated nerves. J Gen Physiol 59:637–658

Hille B (1975) Ionic selectivity, saturation, and block in sodium channels. A four-barrier model. J Gen Physiol 66:535–560

Hockberger PE, Tseng HY, Connor JA (1987) Immunochemical and electrophysiological differentiation of rat cerebellar granule cells in explant cultures. J Neurosci 7:1370–1383

Hodgkin AL, Huxley AF (1952) A quantitative description of membrane current and its application to conduction and excitation in nerve. J Physiol (London) 117:500–544

Horie M, Irisawa H (1987) Rectification of muscarinic K^+ current by magnesium ion in guinea pig atrial cells. Am J Physiol 253:H210–H214

Horie M, Irisawa H, Noma A (1987) Voltage-dependent Magnesium block of adenosine-triphosphate-sensitive potassium channel in guinea-pig ventricular cells. J Physiol (London) 387:251–271

Johnson JW, Ascher P (1990) Voltage-dependent block by intracellular Mg^{2+} of *N*-methyl-D-aspartate-activated channels. Biophys J 57:1085–1090

Keynes RD, Royas E (1974) Kinetics and steady-state properties of the charged system controlling sodium conductance in the squid giant axon. J Physiol (London) 239:393–434

Levi G, Aloisi F, Ciotti MT, Gallo V (1984) Autoradiographic localization and depolarization-induced release of acidic amino acids in differentiating granule cell cultures Brain Res 290:77–86

Lin F, Moran O (1990) Voltage dependent sodium currents in cultured rat cerebellar granule cells. Biosci Rep 10: (in press)

Matsuda H (1988) Open-state substructure of inwardly rectifying potassium channels revealed by magnesium block in guinea-pig heart cells. J Physiol (London) 397:237–258

Moran O, Conti F (1990) Sodium ionic and gating currents in mammalian cells. Eur Biophys J 18:25–32

Nicoletti F, Wrobleski JT, Costa E (1987) Magnesium ions inhibit the stimulation of inositol phospholipid hydrolysis by endogeneous excitatory aminoacids in primary cultures of cerebellar granule cells. J Neurochem 48:967–973

Nilius B (1988) Calcium block of guinea-pig heart sodium channels with and without modification by the piperazinylindole DPI 201-106. J Physiol (London) 399:537–558

Press WH, Flannery BP, Teukolsky SA, Vetterling WT (1989) Numerical recipes FORTRAN version. Cambridge University Press, Cambridge

Pröbstle T, Rüdel R, Ruppersberg JP (1988) Hodgkin-Huxley parameters of sodium channels in human myoballs. Pflügers Arch 412:264–269

Pusch M (1990) Open-channel block of Na^+ channels by intracellular Mg^{2+}. Eur Biophys J 18:317–326

Pusch M, Conti F, Stühmer W (1989) Intracellular magnesium blocks sodium outward currents in a voltage and dose dependent manner. Biophys J 55:1267–1271

Sciancalepore M, Forti L, Moran O (1989) Changes of *N*-methyl-*d*-aspartate activated channels of cerebellar granule cells with days in culture. Biochem Biophys Res Commun 165:481–487

Strata P, Benedetti F (1988) Aspetti di fisiologia del magnesio. EMI, Pavia

White R, Hartzell HC (1988) Effects of intracellular free magnesium on calcium current in isolated cardiac myocytes. Science 239:778–780

Yamamoto D, Yeh JZ, Narahashi T (1984) Voltage-dependent block of normal and tetramethrin-modified single sodium channels. Biophys J 45:337–344